UDC535.39:538.971:669.71:629.11.011.6

Surface Analysis of Aluminum Alloys for Automotive Body Panels

Kaoru Mizuno*1 Yasuo Takagi*1

Abstract:

Several research topics concerning the analysis of surface oxide layers of Al-Mg-(Si) alloys for automotive body panels are discussed. (1) A new method to non destructively estimate the thickness of thin surface layers was developed. This method utilizes one-to-one correspondence between the thickness of the surface layers and their chromatic values (mainly L and/or b*) when the layer is thinner than 50nm. By measuring the chromatic values of the surface with a colormeter, the thickness of the layer can be estimated quickly and nondestructively. This method was applied to estimate the thickness of the MgO layers formed on Al-Mg alloys under various heat treatment processes. (2) The angle-resolved X-ray photoelectron spectroscopy (XPS) depth analysis method was applied to investigate the chemical states of organic contaminants in the surface oxide layers of Al-Mg-Si alloys. The results suggested that hydrophilic groups in the contaminants were chemisorbed to hydroxides in the oxide layers, and formed a kind of metallic soap by subsequent heat treatments. Hydrophobic groups in the contaminants remained at the uppermost surface layers. This phenomenon could be the origin of poor surface wettability. Other topics such as grazing incidence angle X-ray diffraction (GIXD), which was applied to identify the crystal structures of MgO layers of Al-Mg alloys, are briefly discussed.*

1. Introduction

As environmental issues such as global warming have been spotlighted in recent years, aluminum alloys have begun to be used in automotive body panels to reduce overall body weight, therefore improving fuel economy and running performance. High-formability Al-Mg alloys and Al-Mg-Si alloys with bake hardenability are mainly used for this application. It is reported that-heat treating Al-Mg alloys during production causes the diffusion, oxidation and concentration of especially magnesium on their surfaces, forming a relatively thick, island-like film predominantly composed of MgO[1-3]. **Fig. 1** shows the relationship between the elemental distribution in the depth direction of the Al-Mg alloy surface (depth profile) in the Al-Mg alloy production process and in the automobile body manufacturing process. Al-Mg alloy oxide film is formed to some degree during the hot rolling step, thinly elongated during the cold rolling step, and oxidized primarily to MgO during the annealing stage. MgO is reported to reduce weldability and paint adherence[4-8]. With Al-Mg-Si alloys, silicon as well as magnesium is expected to adversely affect their surface properties. The first step toward the

*1 Technical Development Bureau

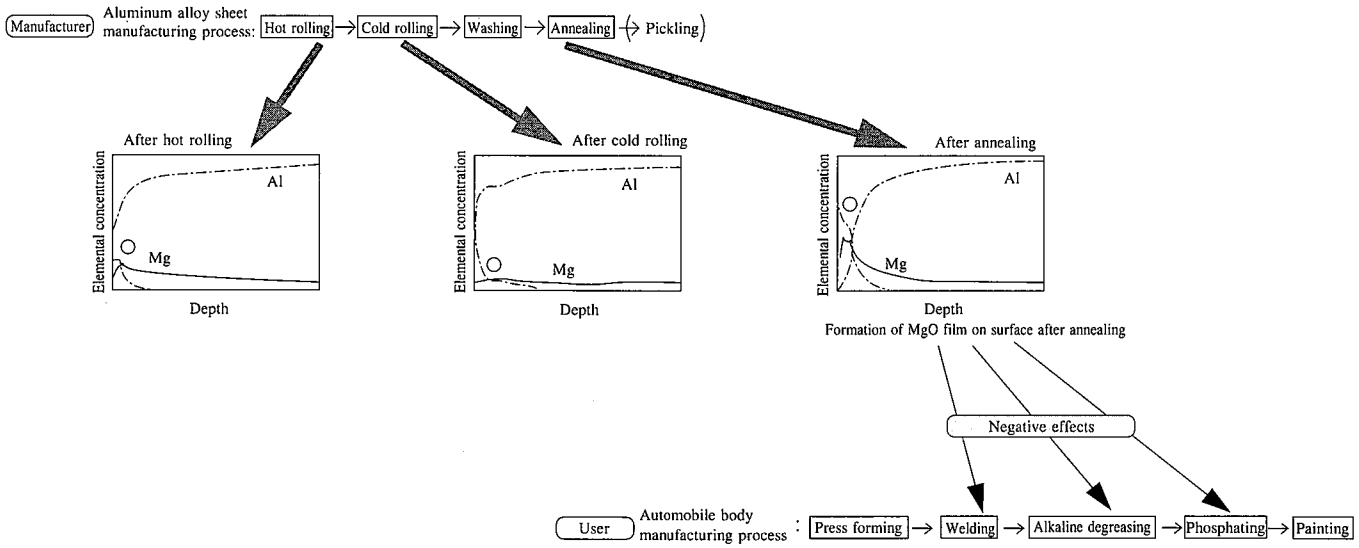

Fig. 1 Schematic depth profiles of the elements on Al-Mg alloy surface in Al-Mg alloy and automobile body manufacturing process

improvement of aluminum alloy performance, therefore, is to obtain findings on the surface state of aluminum alloys by exploiting various surface analysis methods.

X-ray photoelectron spectroscopy (XPS) and Auger electron spectroscopy (AES) have been traditionally used to surface analyze metallic materials. With XPS, information about the chemical state of elements in a relatively wide surface region (several millimeters in diameter) can be obtained. AES is used to perform the elemental analysis of a local region in the order of micrometers in diameter. These methods have chiefly been used to investigate the oxidation behavior of the above-mentioned Al-Mg alloys. Ion beam sputtering can be used to peel the surface to analyze the surface in the depth direction (i.e. depth profiling) and determine the thickness of the oxide film formed there.

This report presents new techniques to analyze oxide films formed on the surfaces of Al-Mg and Al-Mg-Si alloys as well results derived from conventional techniques.

The oxide film on the Al-Mg alloys is known to be relatively simple in composition and to mainly consist of MgO. There is a strong need in industry for the simple and rapid determination of its thickness. Conventional techniques are not capable of simply and rapidly determining oxide film thickness for the reasons that will be described in the next chapter. New methods must be developed for measuring the oxide film thickness of Al-Mg alloys.

The oxide films formed on the surfaces of the Al-Mg-Si alloys are more complicated in composition and structure than those of Al-Mg alloys. Reported here are the results of studies conducted on degreasability and oxidation behavior of these oxide films by using conventional analytical techniques, while focusing attention on their chemical state and local element distribution as well.

2. Simple Method for Measuring Al-Mg Alloy Oxide Film Thickness by Colorimetry

2.1 Background

Oxide film formed on the surface of Al-Mg alloy during manufacturing predominantly composists of MgO. These must be removed by pickling as a requirement for the next automobile manufacturing process, as is shown in **Fig. 1**. In such circumstances, the oxide film thickness must be measured simply, quickly, and nondestructively to control the surface state of pickled Al-Mg alloys. Generally, the oxide film thickness of metals is determined by peeling the surface by sputtering and measuring the depth profile, or by optical methods.

In the former case, XPS, AES, and glow discharge optical emission spectroscopy (GDOES) are used to measure the depth profile. XPS and AES provide useful information, such as chemical state and elemental distribution, but can only make measurements in ultrahigh-vacuum environments. Since specimens must be machined to a size of about 1 cm^2, then placed into a vacuum chamber, XPS and AES are decidedly disadvantageous in terms of speed. Ion beam sputtering is even more disadvantageous. On the other hand, GDOES sputters the specimen at high speed with positive ions produced in a glow discharge plasma and can measure a film of several micrometers in about 20 seconds. GDOES can also provide average information over a relatively wide range ($\sim$mm ϕ), making it suitable for analyzing cold-rolled sheet steel, for example. In the steel industry[9], GDOES is employed in the production control of steel products with thick coatings, such as plated sheets. The authors applied GDOES to aluminum alloys for the first time and showed that it can rapidly measure depth profile of the element on the surface of aluminum alloys[10].

Although GDOES has the above-mentioned advantages, it is still a destructive method similar to XPS and AES. In constrast, the optical methods are advantageous because they can nondestructively measure oxide film thickness. Of these methods, ellipsometry is used in the semiconductor industry to control film thickness. Since surface flatness is required, however, elliposometry cannot be readily applied to specimens with large areas of surface roughness, such as cold-rolled sheet steels. It is also a slow process because specimens must be machined to a size of a few square centimeters.

The authors paid attention to the colorimeter that can measure the intensity of light reflected from the specimen surface when its measuring probe, or a combination of a light source and a detec-

tor, is applied to the specimen surface.

2.2 Color measurement

The color-matching functions $x_i(\lambda)$, $y(\lambda)$, and $z(\lambda)$ shown in **Fig.2** that correspond to the sensitivity of the human eyes are used to quantitatively represent colors. The symbol λ denotes the wavelength of light. From these functions, the tristimulus values X, Y, and Z are defined as follows;

$$X = k\int_{380}^{780} P(\lambda)x_i(\lambda)d\lambda \quad i = 1,2 \qquad \cdots\cdots(1a)$$

$$Y = k\int_{380}^{780} P(\lambda)y(\lambda)d\lambda \qquad \cdots\cdots(1b)$$

$$Z = k\int_{380}^{780} P(\lambda)z(\lambda)d\lambda \qquad \cdots\cdots(1c)$$

where $P(\lambda)$ is the spectral distribution (wavelength dependence of reflected light intensity) of the specimen. The color-matching functions can be regarded as weighting functions at each wavelength.

Color may be measured by the spectral colorimetric method, which measures light from a specimen with a spectrometer, or by a method that reads the stimulus values directly. In the latter direct method, the light is measured in respective wavelength regions by photoelectric sensors with spectral sensitivities almost equal to the color-matching functions $x_2(\lambda)$, $y(\lambda)$, and $z(\lambda)$ and are directly converted into the corresponding tristimulus values X, Y, and Z. With the former spectral colorimeteric method, an entire spectrum is measured in a given wavelength region. It requires an elaborate apparatus, although the measurement are very accurate when a spectrometer is used. The method that directly reads stimulus values is slightly inferior to the former in accuracy, but use of photoelectric sensors in place of the spectrometer makes for a compact apparatus. Portable photoelectric sensors are commercially available and can be used to measure specimens on site without any sampling.

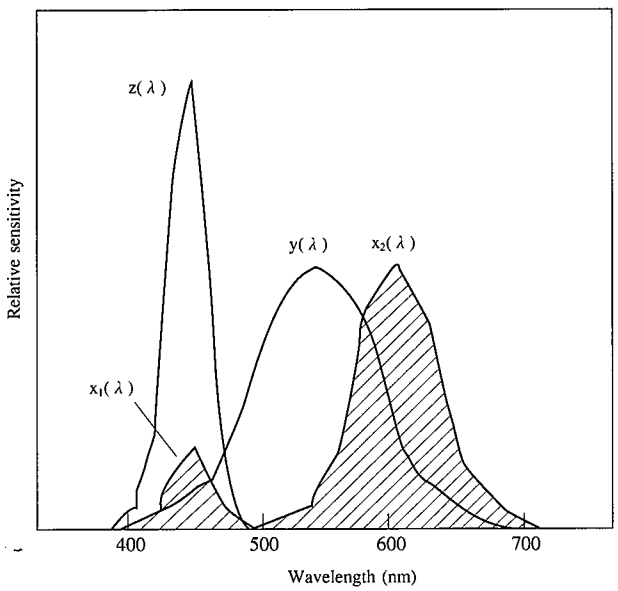

Fig. 2 Color-matching functions

Several methods are available for specifying the color of an object by numerical values. The L*a*b* color notation system is now the most commonly used. The L*, a*, and b* chromatic values calculated by the following equations from the tristimulus values are plotted along the three-dimensional rectangular coordinates to describe a color space:

$$L^* = 116(Y/Y_n)^{1/3} - 16, \qquad \cdots\cdots(2a)$$

$$a^* = 500[(X/X_n)^{1/3} - (Y/Y_n)^{1/3}], \qquad \cdots\cdots(2b)$$

$$b^* = 200[(Y/Y_n)^{1/3} - (Z/Z_n)^{1/3}], \qquad \cdots\cdots(2c)$$

where X_n, Y_n, and Z_n are the tristimulus values of a perfectly reflecting diffuser.

2.3 Experiment with standard samples

2.3.1 Experiments

The chromatic values were measured by a colorimeter (model CR-300, Minolta camera). This instrument consists of a measuring probe and a data processor. The measuring probe houses a diffused light as the incident source (pulse xenon lamp) and three silicon photocells as shown in **Fig. 3**. The specimens chromatic values can be nondestructively measured with this method.

The surface of a cold-rolled sheet of Al-5.5 wt% Mg alloy was mechanically polished. A polycrystalline MgO target was sputtered with positive argon ions by the magnetron sputter deposition method. Thin MgO films were deposited on the substrates by sputtering a polycrystalline MgO target with positive argon ions. The chromatic values L*, a*, and b* of all specimens prepared were measured with photoelectric colorimeter, and the reflected light spectra of some specimens were also measured with a Model UV-245FW, Shimadzu spectral colorimeter and the incident angle was 45°.

To avoid the effect of surface roughness, each substrate was polished with #600 emery paper and mirror finished with a 1-μm-diameter diamond paste. Several MgO films of different thicknesses were formed on different substrates, and their color and spectral distribution were measured. To investigate the effect of surface roughness on the chromatic values of the specimens, 14-nm thick MgO films were formed on each of three different types of substrate, one polished with #120 emery paper, one polished with #600 emery paper, and one first polished with either #600 emery paper and then mirror finished with the diamond paste. The chromatic values of the specimens were measured before and after film formation.

2.3.2 Results and discussion

Fig. 4 shows the reflected light spectra from specimens with

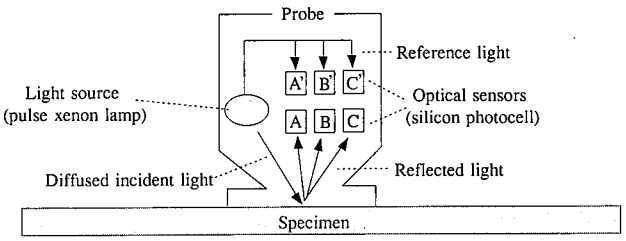

Fig. 3 Schematic illustration of colorimeter (section shown only)

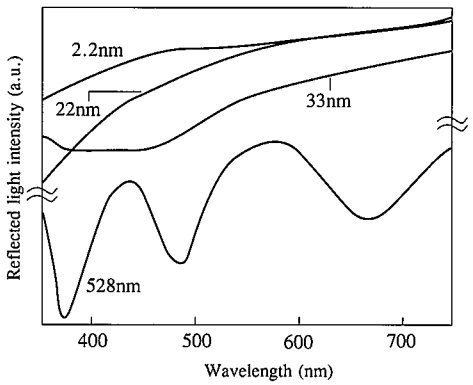

Fig. 4 Reflected light from the MgO film defracted onto the Al-Mg alloy

MgO films of different thicknesses formed on the mirror-finished surface. The single MgO crystals are transparent and absorb little visible light. Since they are deliquescent, they appear slightly yellow when they absorb moisture in air. This is reflected in the fact that the reflected light intensity is low at the short-wavelength side of the spectra of specimens with 2.2- to 33-nm-thick MgO films, which means that shorter wavelengths of light are absorbed more. This is found to increase with increasing MgO film thickness. As the MgO film thickness increases, a rise in the interference effect of light becomes conspicuous. The reflected light spectrum of the 528nm specimen starts to oscillate (i.e. short-wave length end of the 33-nm-thick film and all the 528-nm one.) as shown in **Fig. 4**.

It is expected that the relationship between the thicness of the MgO films and their chromatic values cannot be represented by a simple single-valued linear function. As shown in **Fig. 5**, the values of L* and b* uniquely correspond to the MgO film thickness on the maximum MgO film thickness of about 50 and 30 nm, respectively. In other words, the thickness of the MgO film can be simply known by measuring the L* or b* value in this region. Miyajima and Hashimoto[11] reported that the chromatic values of a transparent thin film can be calculated from its thickness. It was found that a similar tendency is observable for slightly colored films like those of MgO.

Considering that in Eq. (2a) and (1b), the L* value is approximately equivalent to the reflected light intensity near the wavelength of 550 nm on the reflected light spectrum, and in the same way the b* value defined by Eq. (2c) is approximately equivalent to the difference between the reflected light intensity near the wavelength of 550 nm, and that near the wavelength of 450 nm. Therefore, the reflected light spectra of the specimens shown in **Fig. 4** and the tendencies of the L* and b* values shown in **Fig. 5** can be interpreted without contradiction. That is, the decrease in the L* value with the increase in the MgO film thickness in the above-mentioned MgO film thickness of approximately 20 nanometers corresponds to the decrease in the reflected light intensity along the entire spectrum. The increase in the b* value corresponds to the rise in ligh absorption at the low end of the wavelength region with the increase in the MgO film thickness or the rise in the slope of intensity with respect to the wavelength of the spectrum.

Fig. 6 shows the chromatic values before and after the formation of the MgO film on the three types of specimens. The first has the MgO film formed on a substrate polished with #120

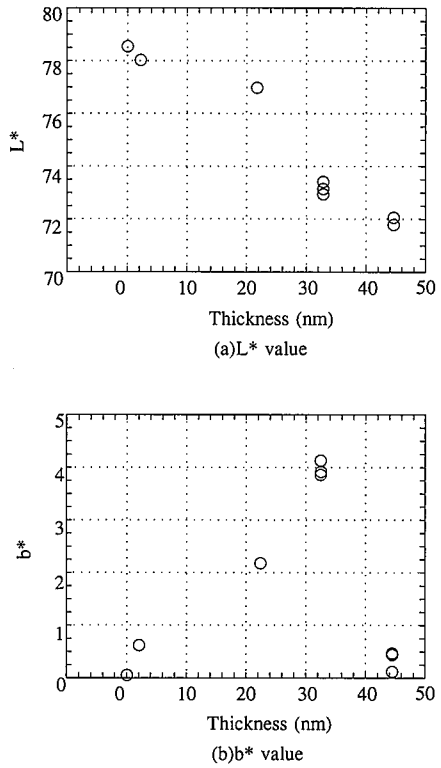

Fig. 5 Relationship between the MgO film thickness and their chromatic values L* and b*

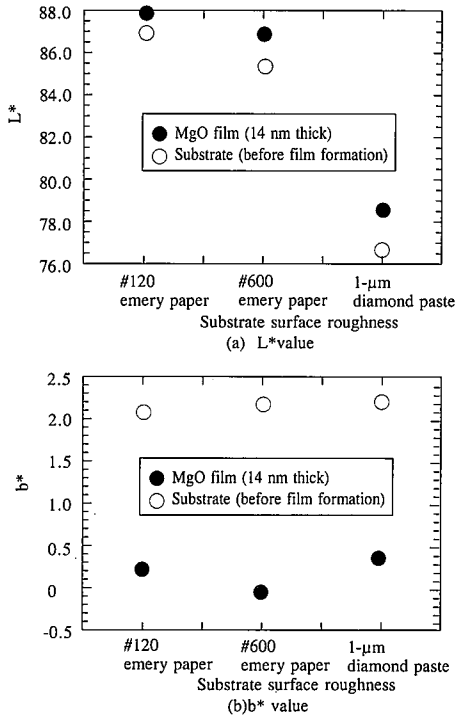

Fig. 6 Dependence of the chromatic values L*and b* on the substrate surface roughness

emery paper, the second has the MgO film formed on a substrate polished with #600 emery paper, and the third was formed on a substrate first polished with #600 emery paper and then mirror finished with a diamond paste. It is evident that the L* value changes more with the polished condition of the substrate rather than with the presence or absence of the MgO film and that the b* value is more sensitive to the presence or absence of the MgO film than to the polished condition of the substrate. These phenomena may be explained as follows. The L* value and the b* value mainly correspond to the reflected light intensity and absorption, respectively, as already noted. Accordingly, the L* value is directly influenced by the reflectivity change while the b* value is insensitive to the reflectivity change and more strongly reflects the absorption of light or interference of light by MgO.

2.4 Evaluation of commercial Al-Mg alloy sheets[12]

As shown in **Fig 7**, the chromatic values of commercially available cold-rolled and annealed Al-Mg alloys vary with an increase of the weight loss of the alloy by surface pickling. This indicates that the oxide film thickness is reduced by pickling. The correlation of the L* and b* values with the pickling weight loss is observed for both shot-blasted Al-Mg alloy sheets, but the correlation of the L* value with the pickling weight loss is not observed for laser-dulled Al-Mg alloy sheets with rough surfaces. This is because surface roughness reduces the reflectivity of light. The b* value is correlated with the pickling weight loss for both laser-dulled and shot-blasted Al-Mg alloy sheets. This means that the degree of pickling for commercial Al-Mg alloy sheets, which is greatly influenced by surface roughness, can be evaluated by the b* value rather than L* one.

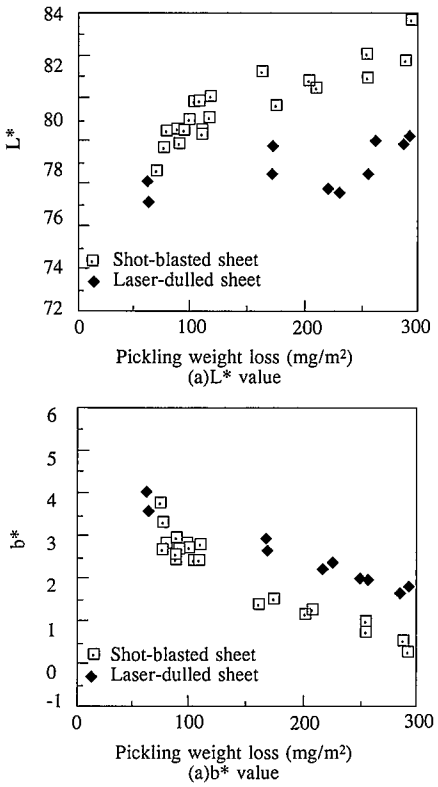

Fig. 7 Relationship between pickling weight loss and chromatic values

3. Analysis of Oxide Film of Al-Mg-Si Alloys

3.1 Previous on oxidation behavior of Al-Mg-Si alloys

As described in the introduction, heat treatment forms an oxide film, mainly composed of MgO, on the surface of Al-Mg alloys. Since the structure and composition are relatively simple in the alloys, its thickness can be measured by the simple methods described in the previous section. It is known, however, the addition of silicon to the Al-Mg-Si alloys forms an oxide film that is considerably different in composition, thickness, and chemical state from that of the Al-Mg alloys. Some of the past studies on the analysis of the oxide film of the Al-Mg-Si alloys are summarized below.

Shulakov et al.[13] annealed the Al-2 wt% Mg alloy and the Al-2.4 wt% Mg-0.48 wt% Si alloy in air, and analyzed the soft X-ray spectra from the specimens. They reported that the oxidation rates of the Al-Mg-Si alloys are lower than those of the Al-Mg alloys, because the silicon and manganese form intermetallic compounds at the oxide film/substrate interface.

Mizuno et al.[14] heated and oxidized the Al-0.9 wt% Mg-0.9 wt% Si alloy after cold rolling and polished it without any solution heat treatment, and analyzed the XPS spectra of the specimens. They calculated the average oxide film thickness and the concentration of positive ions in the film from the spectra. As shown in **Fig. 8**, the thickness of the oxide film increase, and the magnesium concentration in it also rise, while concentrations of aluminum and silicon in it decrease. As reported by Shulakov et al., the Al-Mg-Si alloy was slower to be oxidized than the Al-Mg alloy. They confirmed the enrichment of the metallic magnesium and silicon at the film/substrate interface in the specimen annealed at 300°C for 5 hours (see **Fig. 9**). Using a multipurpose AES-SEM-EDS apparatus, microanalysis was also undertaken to confirm the formation of coarse precipitates a few micrometers in size, such as Mg_2Si and Al-Fe-Si. The depth profiles of the surface of each precipitate and that of the matrix were compared to clarify local differences in oxidation behavior. For instance, **Fig. 10** shows the depth profiles of the matrix, Mg_2Si precipitate, and Al-Fe-Si precipitate in a specimen annealed at 520°C for 2 minutes. The matrix and the Al-Fe-Si precipitate particles are covered with an Al-Mg mixed oxide, while the Mg_2Si precipitate particles are covered with relatively thick MgO. This means that the composition and thickness of the oxide films vary with the composition of the substrate.

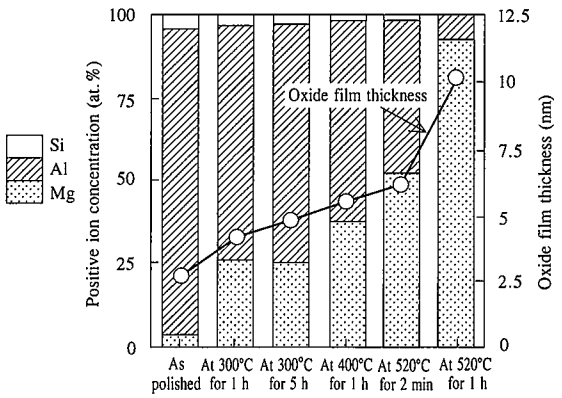

Fig. 8 Dependence of the positive ion cncentration and the oxide film thickness on the oxidation conditions calculated from the XPS spectrum[14]

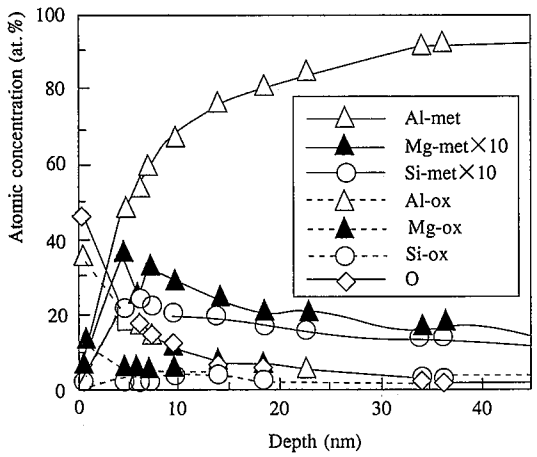

Fig. 9 XPS depth profiles by chemical state[14]
met:metallic; ox:oxide

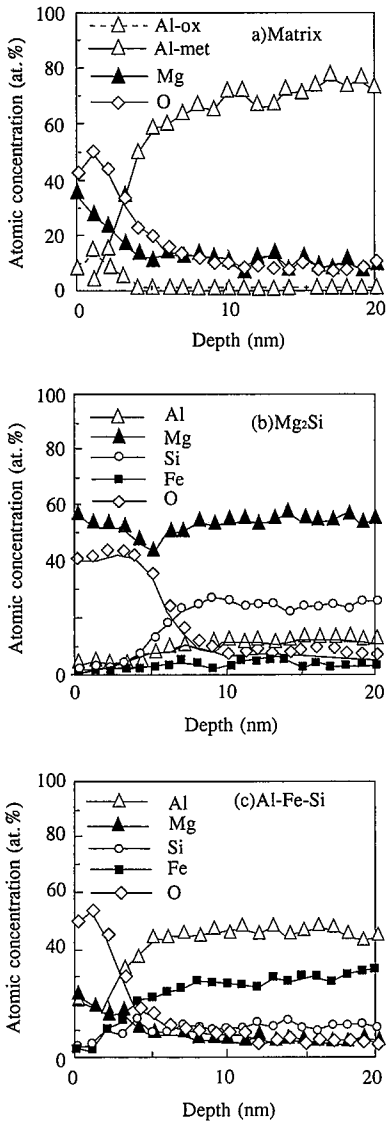

Fig. 10 AES depth profiles of matrix (a), precipitate (b):Mg_2Si, and(c) Al-Fe-Si surfaces[14]

As discussed above, it is clear that compared with the oxide film of the Al-Mg alloys that is predominantly composed of MgO, the Al-Mg-Si alloys' oxide film is more complicated in terms of composition and local elemental distribution.

3.2 Degreasability of oxide film of Al-Mg-Si alloys

3.2.1 Background

In the normal automotive body panel production process, Al-Mg-Si alloy sheets for body panels are degreased and dipped in a surface conditioning solution containing titanium colloid in preparation for the phosphate coating providing good paint adherence and corrosion resistance. Improper degreasing sometimes causes inadequate wetting during the surface conditioning stage. Since this condition is likely to affect the phosphatability of Al-Mg-Si alloy sheets as well, it is important to clarify the relationship between the oxide film and degreasability.

3.2.2 Experiments

Improper degreasing rarely occurs when the oxide film formed during the Al-Mg-Si alloy manufacturing process is almost completely removed by pickling. The quality and thickness of the oxide film are considered to be related to poor degreasability. Although surface roughness are thought to influence the degreasability of commercial Al-Mg-Si alloy sheets, polished sheets were used as specimens to isolate the effects of factors, such as oxide film composition and thickness, that influence the degreasability of Al-Mg-Si alloy sheets. The Al-0.9 wt% Mg-0.9 wt% Si alloy was used as the test material. The material was mechanically polished and finished with a 3-μ m diamond paste, then annealed in an electric oven at 500°C for 2 hours in air. To examine the difference in oil adsorption in the surface between specimens with and without the oxide film, the surface state of oiled specimens without pickling was compared with that of specimens oiled after pickling. Oleic acid ($CH_3(CH_2)_7CH=CH(CH_2)_7COOH$), a fatty acid containing both hydrophobic and hydrophilic groups, was used as model contaminant. The oil was diluted to 1 wt% by using nonpolar n-hexane as the solvent. Specimens before and after pickling were dipped in the solution, removed from the solution, and dried. Some nonpickled oiled specimens were annealed again in air at 150°C for 30 minutes, in order to simulate baking and the tempering process in manufacturing. The specimens treated as described above were finally degreased (ultrasonically cleaned in n-hexane for 10 minutes). Depending on the above preparation conditions, the specimens are designated A, B, and C as follows:

A: Annealed at 500°C for 2 hours, dipped in oleic acid solution, annealed at 150°C for 30 minutes, and degreased;

B: Annealed at 500°C for 2 hours, dipped in oleic acid solution, and degreased;

C: Annealed at 500°C for 2 hours, pickled, dipped in oleic acid solution, and degreased.

The surface state changes of these specimens were analyzed by XPS (Perkin Elmer/Physical Electronics ESCA Model 5500), and 400-W Mg K α radiation was used as the excitation source.

The angle θ between the normal line to the surface of the specimen and the direction of incident photoelectrons to the electron spectrometer was changed to 15°, 45°, and 75°, as shown in **Fig. 11**. The XPS spectra obtained at each angle was compared. If λ is the escape distance of photoelectrons, the detection depth is $\lambda \cos\theta$. The greater the angle θ, the smaller the detection depth becomes. This method, so called "angle-resolved XPS analyzing" is often used for XPS to nondestructively obtain informa-

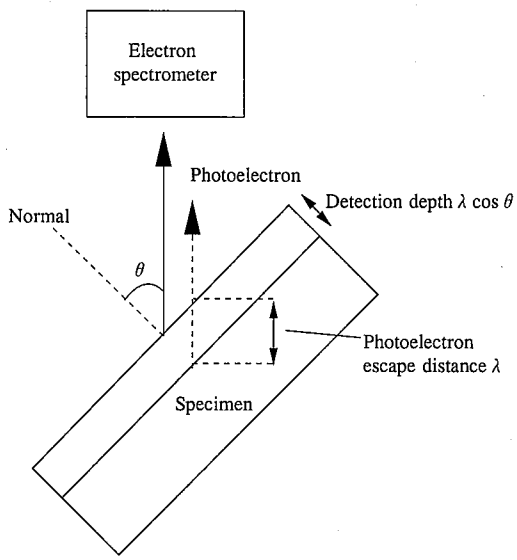

Fig. 11 Photoelectron detection angle and depth in angle-resolved XPS analysis

tion in the depth direction. To know the change in the chemical states of the surface in the depth direction and the orientation of adsorption of oleic acid, spectra were measured at the different ditection angles, θ , 15, 45and 75°.

3.2.3 Results

Elemental concentration at the surface of the specimens, A, B, and C shown in **Fig.12** were calculated from XPS spectra taken at θ =45°. As described in the preceding section, the oxide film formed on the surface of the Al-Mg-Si alloy is locally uneven in both composition and thickness. When the specimen is oxidized in air, the magnesium is selectively oxidized, and at a high temperature (500°C), an oxide film mainly composed of MgO is formed on the surface of the alloy. The relative intensity of the magnesium is low in the pickled specimen C. This means that MgO is considerably removed by pickling. The amount of carbon left after degreasing decreases in the order of specimens A, B, and C. This indicates that the degreasability of the oxide film is improved by pickling and lowered by annealing after oiling.

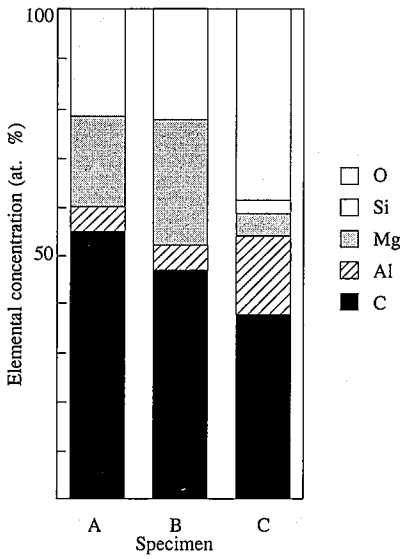

Fig. 12 Change in relative intensity of each element with specimen preparation method (θ = 45°)

Fig. 13 shows measurment taken at various detection angle: θ =15°,45° and 75°. Two types of components of the peak are observed: one derived from the C(O) groups (C-OH group and C=O group) and the other derived from the C-H group. Relative intensity between the components varies with the detection angles on the detection angle θ is seen. The larger the detection angle θ , i.e. the smaller the depth at which photoelectron signals are obtained, the larger the proportion of the C-H group becomes. In other words, the C-H group and the C(O) group are abundantly present at the outer and inner regions of the film, respectively. This suggests that oleic acid is adsorbed with the C-H group and oriented toward the outside and the C(O) groups toward the alloy side. Similar tendencies were observed for specimen B, but specimen A exhibited more pronounced tendencies. With specimen C, which was pickled before oiling, the peak intensity of the carbon is low as shown in **Fig. 12**, and the detection angle (θ) dependency is not evident. The "orientated adsorption" of oleic acid as described above did not occur for specimen C.

The similar angle resolved oxygen 1s peaks are shown in **Fig. 14**. The low energy component of the peak in specimens, A and B derives from the oxygen in the oxide film, (i.e. an inorganic component) while a high-energy component derives from the organic matter in it. The peak intensity of O(C) organic increases with decreasing detection angle. In air, oxides absorb moisture to form hydroxides. Such hydroxides are decomposed in the ultra-high vacuum chamber of the XPS instrument[15]. The proportion of the high-energy component for specimen A, which was annealed after oiling is higher tha that of B. This means that the larger amount of oleic acid is adsorbed on specimen A. Specimen C reveals no detection angle dependence of the O1s peaks, and the peak position corresponds to that of the inorganic component, and no traces were adsorped at the higher angle. This indicates little adsorption of oleic acid occured.

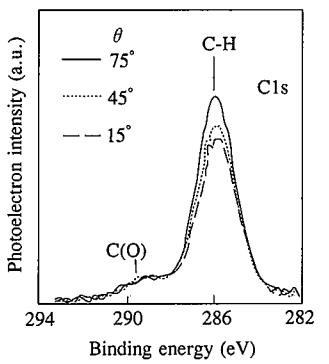

Fig. 13 Detection angle dependence of carbon 1s peaks of specimen A

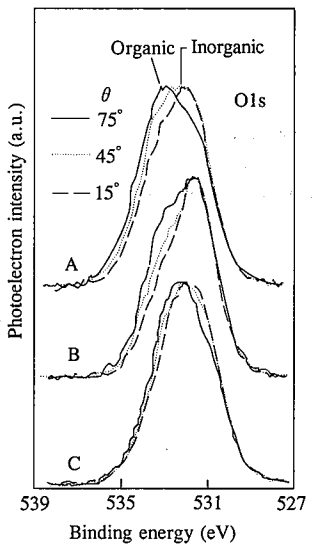

Fig. 14 Detection angle dependence of oxygen 1s peaks of specimens A, B, and C

3.2.4 Discussion

When the specimen is not pickled, the oleic acid is chmisorbed to the oxide film surface due to the strong affinity between the hydrophilic groups in the acid and the oxide film. Part of it has absorbed moisture in the air and formed hydroxides. Such strongly chemisorbed acid cannot be removed easily by the degreasing treatment. Annealing after oiling breaks weak hydrogen bonds to form metallic soap[16], and further lowers the degreasability of the oxide film, as shown in the model of **Fig. 15**. This must be why specimen A surface has the highest concentration of C among the specimens. From these results, it is predicted that when the specimen is oiled without pickling, subsequent paint baking or tempering processes will lower the degreasability of the oxide film. Therefore, some posttreatment to hydrolyze and remove the metallic soap is necessary for restoring degreasability to the oxide film.

4. A New Surface Crystal Structure Analysis Method (GIXD)

The composition, thickness and chemical state of oxide films formed on the surface of aluminum alloy sheets were analyzed for autommtive body panels, and the relationships between these surface properties and the surface performance of the aluminum alloy sheets have been discussed. In this way, considerable findings are being accumulated about the composition and chemical state of the aluminum alloy surface oxide films and about the effects of the composition and chemical state of the oxide film on the surface performance of aluminum alloys. The crystal structure of such oxide films is little known. Oxide film is so thin, conventional techniques to analyze crystal structures like X-ray diffraction cannot be applied to it. It is very likely that the difference in crystal structure between the oxide films has an effect on the adhesive strength, phosphatability, and other surface performance of aluminum alloy oxide films. The crystal structure of single-crystal surfaces has been analyzed by grazing incidence angle X-ray diffraction (GIXD)[17]. An incident X-ray is kept directed at a very small angle to the surface of the specimen and is totally reflected at the surface to achieve a markedly higher X-ray density near the surface, and to increase the diffracted X-ray intensity. GIXD, however, has been rarely applied to polycrystalline materials and such materials that their surface roughness is too large to meet the total reflection condition. In recent years, however, powerful X-ray sources like synchrotron radiation[18] and a high-current rotating-anode X-ray generator[19], and also high-sensitivity two-dimensional detectors like image plates[20] have made it possible to apply the GIXD technique to the structural analysis of oxide films formed on the surfaces of metals such as aluminum alloys. Waseda et al.[21] reported that if the total reflection condition can be satisfied, diffraction peaks from the surface oxide layer as thin as 10 nm from stainless steel sheets can be detected. Takagi and Kimura[22] also succeeded in measuring diffraction beams from an oxide film of about 10 nm thickness formed on the surface of an Al-Mg alloy by using synchrotron radiation as an X-ray source and an imaging plate as an X-ray detector. They identified the crystal structure of the oxide film as nonoriented cubic MgO.

Crystal structure analysis of surface oxide films has just started. As noted above, X-ray sources and detectors have advanced remarkably in recent years and are expected to make great contributions to the structural analysis of surface oxide films. Electron diffraction techniques, such as low-energy electron diffraction (LEED) and transmission electron microscopy (TEM), have also progressed in recent years. They should be used in combination with the above-mentioned GIXD technique.

5. Conclusions

The surface analysis of aluminum alloys for automotive body panels has been described above. Analytical techniques are not yet fully developed in some areas, such as crystal structure analysis. The optimum technique for each application have been developed and applied to the analysis of the surface state of aluminum alloys, contributing to the clarification of the relationship between surface conditions and surface performance of aluminum alloys. The ideal situation will be being able to provide useful information to improve and create the best surface conditions for specific applications of aluminum alloys and other metallic materials.

Acknowledgments

The aluminum alloy samples used in the experimental work reported here were supplied by Sky Aluminum Co., Ltd. T.Koike helped us to obtain the spectra data shown in **Fig.4**. The study described in Reference14) was conducted by one of the authors, K. Mizuno, in the laboratory of Professor Ingemar Olefjord at the Chalmers University of Technology, Sweden. The authors would like to express sincere thanks to those who have provided assistance in their work.

References

1) Field, D.J., Scamans, G.M., Butler, E.P.: Metallurgical Transactions. A18, 463 (1987)

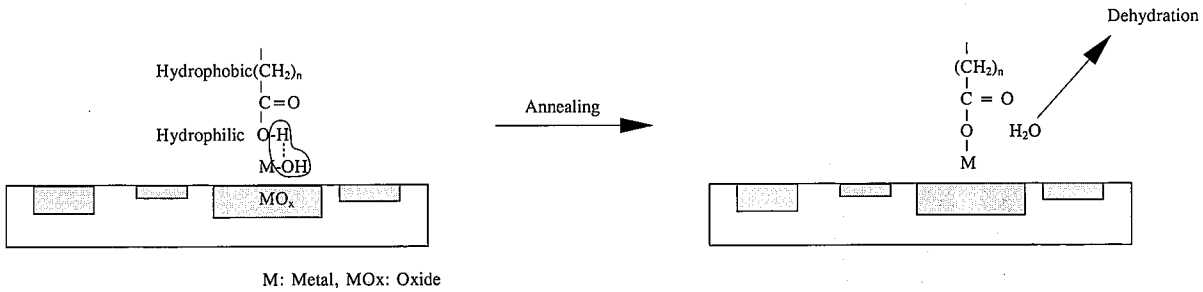

Fig. 15 Model of adsorption of organic molecules on oxide film and formation of metallic soap

2) Lea, C., Ball, J.: Applications of Surface Science. 17, 344 (1984)
3) Wefers, K.: Aluminum. 57, 722 (1981)
4) Ronnht, T., Rilby, U., Olefjörd, I.: Materials Science and Engineering. 42, 329 (1980)
5) Ostgaard, E.: Met. Construct. Feb. 78, (1980)
6) Guminski, R.D., Meredith, F.M.P.: J. Oil Colour Chemists' Association. 44, 93 (1961)
7) Bleisch, G.: Aluminum. 51, 160(1975)
8) Vosskuhler, H., Zeigler, H.: Aluminum. 37,424(1961)
9) Suzuki, K., Yamazaki, S., Mori, T., Ohotsubo, T.: Tetsu-to-Hagané. 72, 565 (1987)
10) Mizuno, K., Takagi, Y., Suzuki, S., Hayashi, K.: Proceedings of 88th Spring Meeting of Japan Institute of Light Metals.(In Japanese), 1995,p.159
11) Miyajima, S., Hashimoto, M.,: Thin Solid Films. 193/194, 748 (1990)
12) Mizuno, K., Takagi, Y., Suzuki, S., Hayashi, K., Kobayashi, T., Kurata, M.: Proceedings of 88th Spring Meeting of Japan Institute of Light Metals.(In Japanese), 1995,p.157
13) Shulakov, A.S., Stepanov, A. P., Brajko, A.P., Muller, H., Kirchmayr, H., Szasz, A.: J. Electron Spectroscopy and Related Phenomena. 62, 351 (1993)
14) Mizuno, K., Nylund, A., Olefjord, I.: Materials Science and Technology. In print
15) Koizumi, M., Takagi, S., Umehara, S.: Journal of Metal Surface Finishing Society of Japan. 37, 503 (1986)
16) Olefjord, I., Nylund, A.: Surface and Interface Analysis. 21, 290 (1994)
17) Robinnson, I.K.: Handbook of Synchrotron Radiation. ed. Moncton, D.E., Brown, G., North-Holland Publishing Co., Amsterdam, New York, Oxford, 1987, p. 221-266.
18) Physical Society of Japan: Synchrotron Radiation. Baifukan, Tokyo, 1986
19) Taylor, A.,: J. Sci. Instr. 26, 225 (1949)
20) Amemiya, Y., Matsushita, T., Nakagawa, A., Satow, Y., Miyahara, J., Chikawa, P.J.: Nuclear Instruments & Methods in Physical Research. A266, 645 (1988)
21) Kosaka, T., Saito, M., Matsubara, E., Waseda, Y.: Transactions of Material Engineering Research Institute, Tohoku University. (In Japanese) 50, 79 (1994)
22) Takagi, Y., Kimura, M.: Private communication, 1995